Spring 5-8-2020

Identification of Human Adrenal Carcinoma Cells Using Photoacoustic Flow Cytometry

Alexis Stahl

IDENTIFICATION OF HUMAN ADRENAL CARCINOMA CELLS USING PHOTOACOUSTIC FLOW CYTOMETRY

A Thesis

Submitted to the Rangos School of Health Sciences

Duquesne University

In partial fulfillment of the requirements for

the degree of Masters of Science

By

Alexis Stahl

May 2020

IDENTIFICATION OF HUMAN ADRENAL CARCINOMA CELLS USING

PHOTOACOUSTIC FLOW CYTOMETRY

By

Alexis Stahl

Approved April 10, 2020

_____	_____
Dr. John Viator Chair, Department of Engineering (Committee Chair)	Dr. Kimberly Williams Associate Professor, Engineering (Committee Member/Reader)
_____	_____
Dr. Fevzi Akinci Dean, Rangos School of Health Sciences Professor of Chemistry and Biochemistry	Dr. John Viator Chair, Department of Engineering Professor of Engineering

ABSTRACT

IDENTIFICATION OF HUMAN ADRENAL CARCINOMA CELLS USING PHOTOACOUSTIC FLOW CYTOMETRY

By

Alexis Stahl

May 2020

Thesis supervised by Dr. John Viator

With consistently high mortality rates in patients with adrenal cancer, lack of early detection and diagnosis are an ever increasing problem in fighting the deadly disease. Currently, very few patients are diagnosed with adrenal cancer within the early stages due to the absence of symptoms until large tumors are formed, which is in most cases is fatal. Because of this, early detection equipment is crucial to optimizing the survival rate in patients. We studied the absorbance wavelength of human adrenal carcinoma cells, as well as the minimum cell concentration needed in samples using photoacoustic flow cytometry (PAFC). PAFC generates ultrasonic waves when particles under flow absorb laser light. Due to the yellow color in adrenal cancer cells, we demonstrate that cells under flow optimally absorb a laser in blue/indigo color. We also determine the minimum number of cells needed per sample to produce a significant

signal within the system. These novel findings will be further used in the future to develop a blood assay for early detection of adrenal cancer cells in the blood stream of patients within a clinical setting, aiding in early diagnosis, and consequentially decreased mortality rates in patients.

ACKNOWLEDGEMENT

I would like to thank Dr. John Viator for helping provide direction and guidance throughout my graduate career and throughout research. He not only helped with clarification and providing critical feedback, but also provided challenging questions and ideas to help me better improve the content. I would not have been able to complete research without Justin Cook, who not only set up the groundwork for this research, but also was a great mentor and research partner, especially when I was first starting in the lab and had to learn everything we were doing. Dr. Kimberky Williams also played a huge role in helping me refine my writing and presentation skills, as well as always being available when I needed help with the content within my thesis.

I'd also like to thank past and present members of Dr. Viator's lab at Duquesne University that I had the pleasure of working with. Specifically, I'd like to give a shout out to Rob Edgar, also played an important role, helping out while he was in the lab by keeping me positive and focused, as well as providing insight and advice when troubleshooting and progressing the research. I'd like to acknowledge those who have done similar research before me for offering valuable perspectives and insight about the subject. Lastly, I would like to thank my friends and family for their constant support and motivation throughout this entire process. Without their frequent words of encouragement and belief in me, I would not be where I am today. I would like to thank my mom for keeping me positive in spite of stressful situations, and my dad for reminding me I can do anything I put my mind to and for keeping me focused throughout this entire process.

TABLE OF CONTENTS

Page

LIST OF FIGURES

Page

CHAPTER 1: INTRODUCTION

Adrenal cancer is one of the rarer forms of cancer, and in return, does not get much attention regarding research advancements. While the exact known number of patients diagnosed each year is unknown, the consequences of the diagnoses are usually deadly. Because of this, early detection is crucial to maximizing survival rates [1]. The adrenals are glands that sit above the kidneys in the abdomen. Adrenal cancer usually develops in the cortex of the adrenal gland and is usually only discovered in patients when found accidentally. Main indicators of adrenal cancer include weight gain, high blood pressure, easy bruising, early puberty in children, and excess facial hair growth in women [2]. However, these symptoms often go unnoticed, making detection difficult due to tumors in the adrenal gland only being recognized when they are already large enough to cause abdominal issues (Fig. 1) [2,3].

Figure 1: The average cancerous tumor within the adrenal gland is 5-6cm, approximately the size of the tumor above. However, tumors can go unnoticed until much larger, with tumor size ranging between 3-40cm [2-3]

Early detection of adrenal carcinomas is statistically more difficult than that of other cancer types due to the rarity of the cancer itself and lack of noticeable symptoms within the patient. Not only is the presence of the cancer uncommon, but due to it being so uncommon, early detection is also uncommon. Only about half of the people with adrenal cancer produce symptoms due to the hormones made by the tumor, the rest only notice symptoms because the tumor has grown large enough to press on nearby organs [4,5,6]. The cancer is easier to detect in children due to the tumor secreting androgens or estrogens into the body. Androgens are male-type hormones, while estrogens are female-type hormones. This causes children to grow excessive hair, enlarge sex organs, and can cause puberty to onset earlier [2,3]. While these hormones produce noticeable symptoms in children, adults have already gone through puberty, making these increasing levels of sex hormones less noticeable, and consequently these levels go unnoticed, repressing symptoms until the tumor grows quite large, making detection easier but treatment difficult. However, this is different in rare cases where tumors in women produce androgens, and tumors in men secrete estrogens. This will cause more noticeable symptoms, as men will develop enlarged tender breasts, and women will notice excessive facial hair and a deeper voice [2,3]. Regardless, the majority of adrenal cancer patients present only at a more advanced stage when fatality is, unfortunately, likely.

It is estimated that around 400 people are diagnosed with adrenal cancer each year and is found most commonly in middle aged adults. The average age of someone diagnosed is 46 years of age, however, they can be found at any age [2,3]. Early detection to this type of cancer is essential because if the cancer is diagnosed and treated before spreading outside of the adrenal gland, the 5-year survival rate is about 65% [7,8]. A 5-

year survival rate is an estimated percent of the number of people who will live at least 5 years after the cancer is detected. Only 30% of adrenal cancers are currently diagnosed at this stage, making the overall survival rate very low. The majority of adrenal cancer is found at more advanced stages, making the 5-year survival rate range from 44% to as low as 7% in extreme cases [7,8]. Due to these statistics, it is apparent that earlier detection and testing needs to be done to increase longevity in patients.

1.2 ANATOMY

The adrenal gland is found on the posteromedial surface of the kidney and is composed of an outer cortex and an inner medulla, all surrounded by a connective tissue capsule [9,10]. The adrenal glands are very close to many other major organs within the body, making it easier for the cancer to spread to other areas quickly. Because of this, it is important that when treating adrenal cancer that the cancer originated from the adrenal cells and did not spread from other areas, making the cells different in structure and function. It is also important to ensure fast and early detection of this cancer before the cancer metastasizes to other organs, decreasing the 5-year survival rate to only approximately 36% [11]. These glands produce hormones that respond to stress, help regulate your metabolism, immune system, blood pressure, as well as many other essential daily functions [10].

The cortex of the adrenal gland originates from the embryonic mesoderm and secretes two cholesterol packed hormones: corticosteroids and androgens. These two hormones are believed to cause adrenal cancer cells to have increased levels of cholesterol than other cells. Because of this, studies have been done to investigate the

use of cholesterol as a novel marker for the photoacoustic detection of adrenal cancer tumor cells [12,13,14]. These studies lead us to believe the high concentration of cholesterol can be considered targeted when running adrenal cancer cells through a photoacoustic flow cytometer

Inhibitors of cholesterol have been developed initially as therapeutics for cardiovascular disease to target reducing the building of cholesterol esters in macrophages, but studies in animals show the presence of adrenal toxicity, which has led researchers to consider the inhibitor for use in adrenal tumors [15,16]. These inhibitors stop these toxic tumor cells from producing more cholesterol, and in return in mechanistic trials has caused stress in the tumor cell which leads to cell death. It has been well accepted that cancer cells need excess cholesterol and intermediates of the cholesterol biosynthesis pathway to continue increasing rapidly, which further supports the idea of using cholesterol for photoacoustic detection of adrenal cancer cells.

Figure 2: This figure shows the adrenal glands within the human body, highlighted in orange. Due to closeness in proximity to many other major organs, this rare form of cancer can metastasize to other major areas, drastically decreasing the 5 year survival rate and chance of remission [9-11].

1.3 PHOTOACOUSTCIS

Photoacoustics is known as the production of acoustic waves by light absorption [20]. This effect occurs when an acoustic wave is excited through the interaction of electromagnetic waves with matter. The photoacoustic effect relies on thermoelastic expansion, usually with the use of a pulsed laser light. When the laser hits the sample, the energy from the laser is absorbed by some of the molecules within the sample, causing the temperature to increase. This temperature increase causes the molecules to expand, giving off a pressure wave [20]. However, the pressure must oscillate in order to generate a sound wave, which is why the laser pulses rapidly at average frequencies around 1-100MHz, which is between 50-5000 times higher than the human ear can detect [21,22]. This wave is detected by a transducer and processed by an oscilloscope, which displays the acoustic waveform as a visible waveform on its display screen [23].

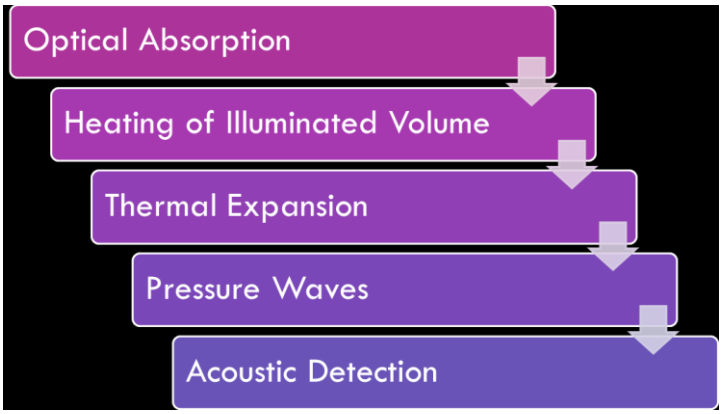

Figure 3: How to evaluate an acoustic signal.

Various techniques can be used for the excitation, generation, and detection of the photoacoustic signals. By periodically heating and cooling the sample, pressure fluctuations are created, which generate acoustic waves sensitive enough to be detected by transducers [24-28]. This excitation can occur as modulated excitation or pulsed

excitation. Modulated excitation uses radiation sources with fluctuating intensity in the form of a sine or square wave. This typically results in a 50% duty cycle, which is the fraction of time in which the signal is active. This can be overcome by modulating the phase of the radiation that is emitted [24-28]. Pulsed excitation uses laser pulses to excite the sample, pulsing with durations of a few nanoseconds, which causes a short illumination of the sample followed by a longer dark cycle. This is what causes the thermal expansion in the sample, and the signal is processed by oscilloscopes [29]. Thermoelastic expansion can be described as energy that is quickly absorbed by a chromophore such that the resulting localized heating causes rapid expansion of the chromophore that proliferates as a pulse of acoustic energy [29]. To excite one frequency, laser beams and a modulated excitation is best, but to excite a multitude of acoustic waves, laser pulses are the optimal choice.

The signal of the acoustic wave can be generated either directly or indirectly. Using a modulated or pulsed laser inside a solid, liquid, or gaseous material is considered direct generation. This means detection takes place either at the surface or inside the sample [30-33]. When the laser excites the sample inside the cell, the sound waves can be detected using a microphone. This signal has an amplitude, defined by,

$$p = FW_0\mu_0$$

Where,

W_0 = Incident radiation power

a = Absorption coefficient of the sample

F = The proportionality factor

and cell constant defined as F can be calculated by,

$$F = G\,(\gamma - 1)\,L/\gamma V$$

Where we define each coefficient as,

G= Geometric factor of the order of one,

γ = Adiabatic coefficient of the gas,

L = Length of the cell

V= Volume of the cell.

Photoacoustic signals are indirectly proportional to the modulation frequency and the cross section of the cell [30-33]. As the cell decreases in size and modulation frequency, the signal increases. The modulation can be defined as,

$$\omega = 2\pi v$$

As mentioned previously, short laser pulses are used for direct photoacoustic generation. This leads to an expansion of the sample, creating pressure pulses. These pulses can be detected directly by optical methods or piezoelectric transducers. The depth resolution of this phenomenon depends on the time resolution of the transducer, which can be calculated by multiplying the speed of sound on the sample with the product of the temporal resolution [30-33]. The depth can range from micrometers to centimeters, depending on the absorbance and scattering of the sample. If samples are not measured directly, they can be measured indirectly by heating the sample to create excitation, and then transporting the heat to the interface of the sample This is described as a thermal wave [30-33]. This method is only used in the analysis of condensed matter and is used less frequently than the direct method.

The photoacoustic effect has many advantages, one of which being that the pressure waves are detected and generated directly by absorbed energy. This can be

compared to absorption spectroscopy, where samples are excited by electromagnetic radiation. The absorbencies are detected indirectly from either reflectance or transmittance [34-35]. Photoacoustic imaging provides a higher resolution of ultrasound than other optical imaging, while also maintaining the contrast attainable within the optical imaging, proving to be an advantageous method in adrenal cancer cell detection.

1.4 BLUE LASER LIGHT HYPOTHESIS

To determine whether or not cholesterol is a novel marker for photoacoustic detection of adrenal carcinomas, it is important to note that cholesterol gives off a yellow color [17,18]. This yellow color is also prominent within the adrenal cortex, meaning that there is an excess of cholesterol within the adrenal cortex of adrenal carcinomas [17,18]. This color is important when considering photoacoustic flow cytometry due to the idea that the targeted cells can absorb specific laser energy and produce an acoustic response. When considering the color spectrum, yellow/orange reflects red and green light, and absorbs blue/indigo light [19]. With this in mind, it is important to note that the color spectrum is a subset of the electromagnetic spectrum. This consists of a range of frequencies of all different energy waves. Since photoacoustic flow cytometry uses a pulsed laser system, blue lasers would be best absorbed by the yellow adrenal cancer cells within the flow chamber, producing an acoustic wave that signifies the detection of the cell. The optimal wavelength for indigo/blue colors is between 425-450nm [19], which in theory is the optimal detection range for adrenal cancer cells within the photoacoustic flow system.

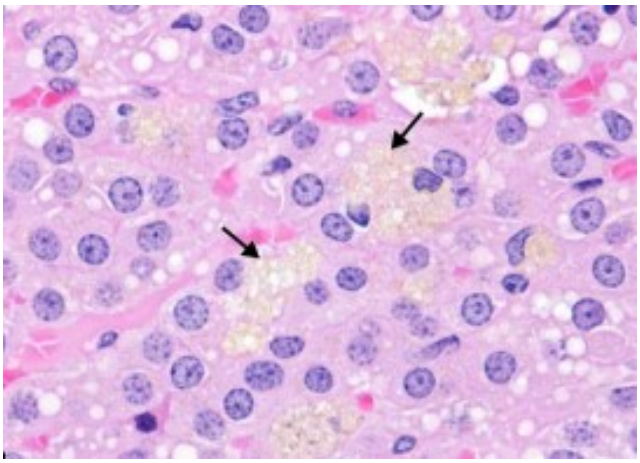

Figure 4: Adrenal gland, Cortex – Pigment in a male F344/N rat from a chronic study. Discrete, foamy cells in the inner cortex (arrow) contain yellow-brown pigment. [19]

Since the optimal detection range for adrenal cancer cells using a photoacoustic flow system is believed to be 425-450nm, these are the points that are the main focus when running experimental trials. At these levels, an indigo/blue laser pulses at the cells within a flow system, and if there is a detection a noise will produce a signal on the oscilloscope that is hooked up to the flow system. In order to fabricate a photoacoustic flow system for adrenal carcinoma detection, it is important to first determine the optimal wavelength to detect the adrenal carcinoma cells, giving vital information on the specifications of the flow system, as well as discovering novel information about the detection wavelengths of the cells themselves.

1.5 HISTORICAL AND CURRENT INVESTIGATIONS

The original physical effect of photoacoustics was discovered by Alexander Bell in 1878 [36]. After inventing the telephone in 1876, he began experiments to adapt the photosensitivity of selenium to telephone transmission. Bell and his assistant, Charles Sumner Tainter, were able to wirelessly transmit voice messages in June 1880.[37-39] In

August of 1880, Bell presented the *Photophone*, consisting of a transmitter made up of a thin silver glass disk on a frame, which a flexible rubber hose with a mouthpiece attached[37-39]. When the sun hit the mirror, the optics arranged so that the reflected light is absorbed by a receiver, creating a telephone circuit as seen in Figure 5. When someone spoke into the mouthpiece, the mirror vibrated which causes fluctuations in the light intensity at the receiver. This light intensity is converted into sound in the telephone circuit, allowing the user to hear what the other person spoke into the system. The photophone created by Bell is considered the first optical communication device, and the beginning of the advancement of photoacoustics.

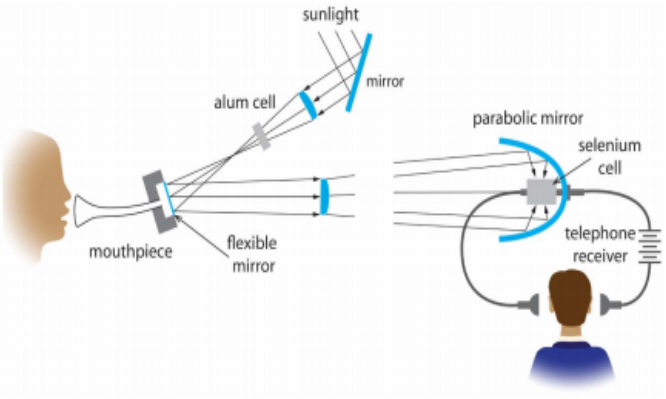

Figure 3: Image of how the Photophone designed by Alexander Bell and Charles Tainter operates. Considered the first optical communication device, the first voice message transmitted by these means was over 213 m in Washington D.C. in June 1880 [36].

Bell's discovery also suggested that when different solid substances are illuminated with a beam of light energy, acoustic energy at the same frequency as the first frequency is created [36] . Later, in April of 1881, Bell created a more advanced communication device, replacing the selenium-cell from the photophone with a lamp-black receiver. This receiver directly converts the light into speech with distances up to 40m [38]. These discoveries caused many other notable scientists to conduct more

experiments in this area. For example, also in 1881, Lord Rayleigh determined that the sounds can be explained by the vibration due to unequal heating of the plates when illuminated with the intermittent light. [40] Wilhelm Röntgen and John Tyndall also shared that heating and cooling of the air in thermal contact with the disk is the cause for sound production, also discussing how this idea can also take place with the absorbtion of vapor and gas [41-42].

Advancements within photoacoustics halted for over fifty years until a technology for infrared gas analysis was created by Mark Veingerov. After studing the work done by Röntgen and Tyndall, he published a paper in 1938 on a method of gas analysis based on the optico-acoustic Tyndall-Röntgen effect [43]. Within this paper, Veingerov used capacitive microphone diaphragms and a Nernst flower as an infrared source to detect CO_2 concentrations in N_2 down to about 0.2 vol. % [43-44]. In 1948, August Herman Pfund introduced a similar system for use at Johns Hopkins Hospital which detects CO and CO_2 gases. His system measured changes in gas temperature using a thermopile covered from direct radiation, which avoided the need for acoustic noise isolation [45].

With the development of the laser in 1960, there was renewed interest in gas analysis. The laser allowed for reproducibility, spectral purity, high stability, and ultralow gas concentration detection and analysis. These types of lasers were used in 1968 by E. L. Kerr and J. G. Atwood, who developed laser-illuminated absorptivity spectrophones for gas analysis. One used a pulsed ruby laser, and the other uses a chopped CW CO_2 laser, detecting acoustics using a capacitance microphone [46]. In 1971, Lloyd Kreuzer developed a chopped He-Ne laser excitation within a cell using an electret microphone, showing ultra-trace detection at ppb levels [47]. Meanwhile, Anders

Jonas Ångström measured the thermal diffusivity of solids by heating a rod periodically and noticed temperature fluctuations, marking the first foundation of thermal waves [48]. This is important in the development of photothermally induced sound waves, introduced by Allan Rosencwaig and Allen Gersho in the mid-1970s. This development has been widely utilized in thermal wave microscopy applications [49-50].

In 1973, Rosencwaig began more investigations of Bell's effect in solids along with William Harshbarger and M. B. Robin. Within Harshbarger and Robin's paper, they continue the use of the word "optoacoustic," while Rosencwaig coins the term "photoacoustic" for the first time [51-52] . While both parties use similar instrumentation in their papers, Rosencwaig uses photoacoustic in order to "avoid any confusion that may result between the original optoacoustic and acousto-optic" [53]. The acousto-optic effect discusses diffraction of light by acoustic waves in a crystal. This technique was further studied in several other experiments by Rosencwaig, including the spectroscopy of biological materials such as cytochrome and hemoglobin [53].

Bell Telephone Laboratories Inc. re-emerged with the first ever imaging studies on inorganic media such as non-destructive evaluation of surface flaws and subsurface inhomogeneities, which has become a big commercial success within photoacoustics. This experiment also paved the way for the studies done by M. Luukkala and A. Penttinen, who used a low-frequency photoacoustic system to get a 5 μm resolution image of a mask structure for an interdigital acoustic-surface wave transducer on a photographic glass plate [54]. Hemantha Wickramasinghe then demonstrated the imaging of acoustic impedances using a high-frequency acoustic microscope that was modified for photoacoustic studies in 1978[55].

Photoacoustics was introduced into the biomedical field in 1964 when short light pulses were done on the eyes of a living rabbit by L. Amar *et al.* using a ruby laser running in normal mode. This laser produced an average of 50mJ pulses of 1 μs duration in a pulse train of 400 μs. The detector showed acoustic transients that correspond to each of the laser pulses as shown in Figure 5. These waves detected were not shock waves, but elastic wave trains that carried a main frequency around 40KHz [56]. This study caused multiple other scientists to study more on laser-induced acoustic transients in the eye, mainly to investigate damage to the retina caused by lasers.

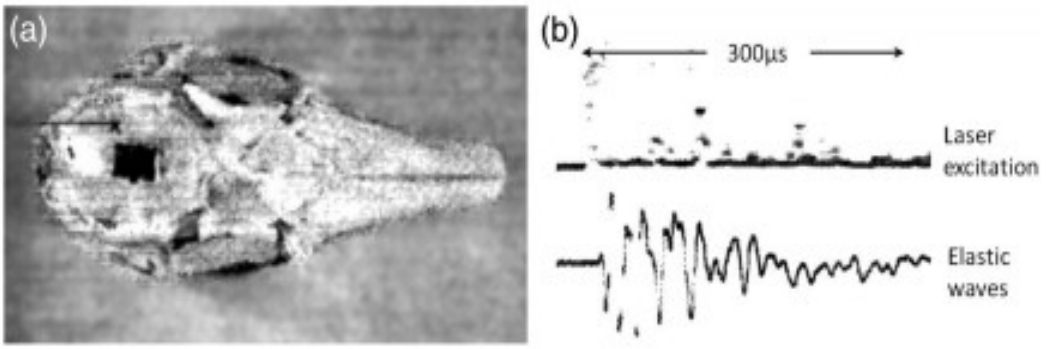

Figure 4: First photoacoustic traces from biological sample. (a) Photograph of rabbit used in experiment; (b) using a pulsed ruby laser and piezo-electric detector, these opto-acoustic tracs are obtained [56]

With the advancement of technology, Rosencwaig and others investigated on biological samples to determine the extent of drug incorporation into skin, measuring the photoacoustic spectra of skin to find changes in optical absorption due to the presence of the drug [57-58]. Then, Theodore Bowen introduced the idea of imaging soft tissues using this method in 1981. Bowen and coworkers determined that a practical thermoacoustic imaging system was possible, and that the method using non-ionizing energies provided information complementary to conventional imaging methods, such as echography, x-ray imaging, and nuclear isotope imaging [59]. Bowen and colleagues also

introduced thermoacoustic A-scans excited using electric currents with copper electrodes inserted in a two-layer phantom comprising muscle-tissue-mimicking layered samples topped with vegetable oil, and thermoacoustic A-scans excited using low-intensity pulses from a 2.45 GHz magnetron source, from interfaces of a variety of materials including a material comprised to simulate the properties of lipids, bone, and muscle [60].

In 1993, Alexander Oraevsky *et al.* created a theory to determine tissue optical properties by acoustic detection of laser-induced stress waves. The authors used a lithium niobite acoustic detector and a Q-switched Nd:YAG laser pumping second and third harmonic crystals to give 1064, 532, and 355 nm wavelengths on various unknown biological tissue samples [61-62]. Oraevsky *et al.* also stated that this method could be used to see the absorbed optical energy in turbid media and is applicable to layered tissues. This is referred to as the laser-based optoacoustic technique. Vivek Srinivasan *et al.* studied the hemoglobin and water concentration, oxygen saturation, and scattering measuring *in vivo* by near-infrared breast tomography in 2003, and photoacoustic imaging in cancer detection and diagnosis is studied by several researchers in 2011 [63-65].

John Viator and coworkers showed the first basic ideas for photoacoustic flow cytometry, doing testing on a photoacoustic probe for depth determination in 2002 and studied the photoacoustic and reflective methods of epidermal melanin content in 2004 [66-67]. John Viator and Weight later became the first researchers to study the photoacoustic detection of melanoma cells in the circulatory system using photoacoustic flow cytometry in 2006, leading the way for all of the photoacoustic imaging and cancer detection studies that are being tested using similar methods today[68-70] In July of

2012, Ekaterina I. Galanzha and Vladimir P. Zharov developed another basic idea for the photoacoustic flow cytometry method used today. Their research overviewed that unique applications of photoacoustic flow cytometry focused on ultrasensitive detection of normal blood cells at different states, as well as rare abnormal cells such as circulating tumor cells and cancer stem cells. They also discussed how their novel advancement gives the opportunity for dynamic studies of blood rheology, something otherwise impossible [70]. Galanzha emphasizes that his system is also helpful in providing early diagnosis for cancer, infection, and cardiovascular disorders, meaning this system has helped pave the pathway to much of the current research regarding photoacoustics and early detection of many deadly diseases.

One current investigation is, *In vivo liquid biopsy using Cytophone platform for photoacoustic detection of circulating tumor cells in patients with melanoma*, which was published in June of 2019. The paper focuses on demonstrating the high sensitivity of the Cytophone technology using an in vivo photoacoustic flow cytometry platform for label-free detection of melanin-bearing circulating tumor cells in patients with melanoma. The photoacoustic methods developed by Viator and Galanzha *et al.* can be used directly on patients with melanoma, which lets the researchers detect small amounts of circulating tumor cells in vivo and destroy them using laser pulses. [71]. Another current investigation includes the, *Bacteriophage-mediated identification of bacteria using photoacoustic flow cytometry,* which focuses on developing a method to determine the bacterial content within blood samples using dyed bacteriophage being process through a photoacoustic flow cytometer. A schematic of the system created can be seen in Figure 6 below, which is similar to the system being used within this research.

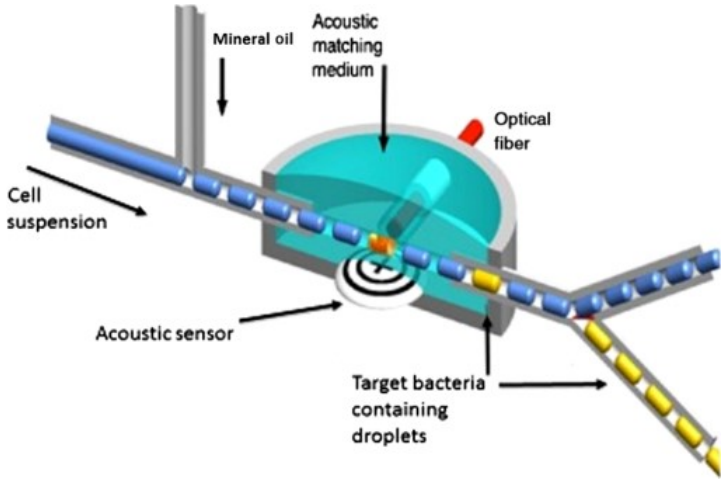

Figure 5: Schematic of photoacoustic flow chamber with parts labeled for identification [72].

All of this research shows the development of photoacoustics in biomedical systems, with substantial use of photoacoustic flow cytometry in current studies. Without the development of photoacoustic flow cytometry, the current advancements discussed would not be possible, making early detection of many diseases much harder than it has come to be. While the previous work provides good background for the work done within this study, these systems do not have the capabilities to detect adrenal cancer cells. As of now, there is a lack of published work regarding early detection of adrenal cancer cells using photoacoustic flow cytometry, making detection of adrenal cancer cells using a photoacoustic flow cytometer a novel advancement.

1.6 PURPOSE

Despite the increased research regarding photoacoustics and various cancer and disease types, there has yet to be research including adrenal cancer. This can be highly attributed to how rare adrenal cancer is, averaging less than 400 diagnosed cases each year. The main goal of this study is to identify lab grown adrenal cancer cells within a photoacoustic flow cytometer. Due to the lack of known characteristic traits about

adrenal cancer cells, fabricating an acoustic flow system to accommodate them requires testing to quantify current unknown traits. Without this knowledge, we cannot properly calibrate a laser to pulse at the cells and provide the results desired. While previous work introduces the basic mechanical setups of photoacoustic flow cytometry with respect to other cancer and disease types, there has yet to be work incorporated into the characteristics of specifically the adrenal cancer cell, which we must first determine before fully fabricating and clinically testing these cells using a photoacoustic flow cytometer.

The goal of this study was to investigate the optimal laser wavelength absorbed by the adrenal cancer cells and determine a current cell concentration detection limit for the flow system. By determining the optimal wavelength range, we can calibrate the laser to be used for the flow system to pulse at the cells at that wavelength, therefore showing the detection, or lack of detection on the oscilloscope. At the same time, by determining the cell concentration detection limit, we can determine how many cells must be within the sample for the laser to detect its presence. In clinical samples, this detection limit can account for how advanced the adrenal cancer is within the patient, and therefore act as an aid in their diagnosis as well.

One way to determine the cell concentration and wavelength limits is by setting up the flow system and running several tests. The first test focuses on the calibration of the laser, and another test focuses on the number of cells flowing at a time. The calibration of the laser must come first, since these test results will not only prove that there is a detection but will limit the range at which the detection is located, which makes further tests simpler and less time consuming. The next study focuses on the minimum

number of cells that can be detected, decreasing the number of cells in each sample until there is no noticeable detection in the ranges previously determined. This study investigated the optimal range of wavelengths the adrenal cancer cells were detected at, and the minimum number of cells that must be present in the sample to warrant a detection. This study also hopes to prove the detection range is detecting the cancer cells by comparing the graphs of the cancer cells to that of other various samples that are ran through the system in future studies.

The results from this study will be further used to develop a blood assay, distinguishing circulating adrenal tumor cells from other cells in the blood stream. This will require various further investigations, including studying other cells in the blood stream to ensure they are not detected, as well as determining cell separating techniques to successfully extract the target cells from the blood stream. These future tests will further improve the accuracy of the system, as well as provide real-time results using just a simple blood test.

CHAPTER 2: METHODS

Determining the detection and dilution limits of the adrenal cancer cells requires multiple various processes, including culturing the cells for growth and testing, fabricating a working photoacoustic flow system, testing the cells within the newly created flow system, and running all data from the flow system through a data analysis so that it can be determined if the signals received during testing are significant, showing the system is detecting the adrenal cells at a quantifiable number. These multi-step tests are run to determine if adrenal cancer cells can be detected, and if so at what absorbance

wavelength. These tests also determine the concentration of cells that are required in each sample for a detection to be present. Both of these characteristics will then be set within the flow system created, which will then be used for further testing and fabrication of a photoacoustic flow system for use to aid in the detection and diagnosis of adrenal cancer in a clinical setting.

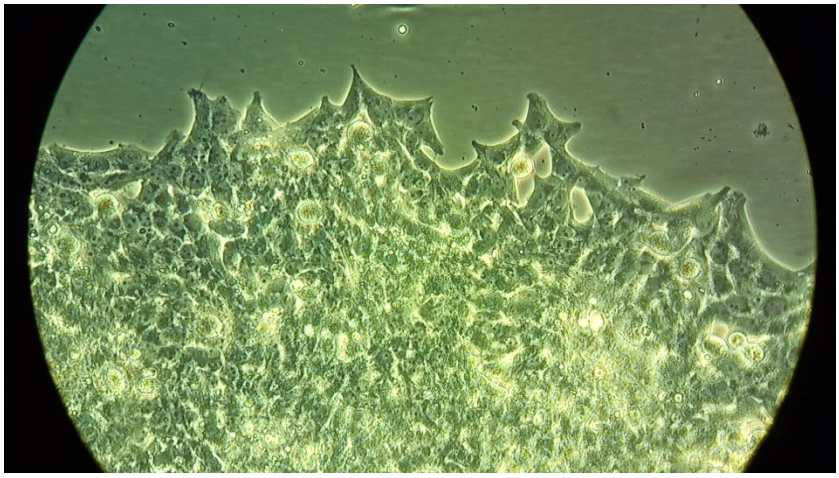

Figure 6: Photo of adrenal cells grown in the lab to be used for testing.

Due to the lack of research in the area, there is currently no photoacoustic system that tests for adrenal cancer cells, as well as there is not much information on the cell characteristics needed to successfully implement the design as well. This affects testing because not only do the detection and dilution limits need to be determined, but the calibration and entire setup of the system must be tested as well. This can prove difficult, as there is no known value that can serve as a constant in all of the testing. Because of this, the flow system is provisionally set up first. and adjustments are made at the same time as the detection limit is determined While both of these are being tested, the cell sample concentration is 10^6 cells/ml to provide a constant. Once adjustments to the machinery is made and a detection limit is determined, both stay constant while the cell

concentration limit is then tested. To determine that all 3 unknowns are found and work consecutively, cells from other cancer types will be run through the system using the same calibrations to show that only the adrenal cancer cells are detected using the newly found characteristics, and that other cancer types will not signal a detection within the system.

2.1 CELL CULTURE

In order to run the detection threshold of the adrenal cancer cells and determine a current dilution detection limit tests, an abundance of cells must be grown to be tested on. When determining which strain of cells to grow, NCI-H295R Human Adrenal Carcinoma cells were chosen due to their ----rapid growth rate. Cells were suspended in 4ml of cell media made up of Nu-Serum 1, ATCC-formulated DMEM:F12, and ITS+ Premix consisting of insulin, transferrin, selenium, BSA and linoleic acid and stored in an incubator. The media was changed every 4 to 5 days until substantial clusters of cells were seen when viewing the flask under a microscope. Each flask of cells was then flushed with trypsin and additional cell media to separate the cells from the flask, where they were then spun down into a pellet using a centrifuge and resuspended in 3ml of cell media. 2ml freezer vials were then filled with 1ml glycerol and 1ml of the cells in the media and placed into a freezer set to -80 degrees Celsius. Protocols for cell cultures can be found within the appendix, giving further detail on the steps needed to grow the cell cultures.

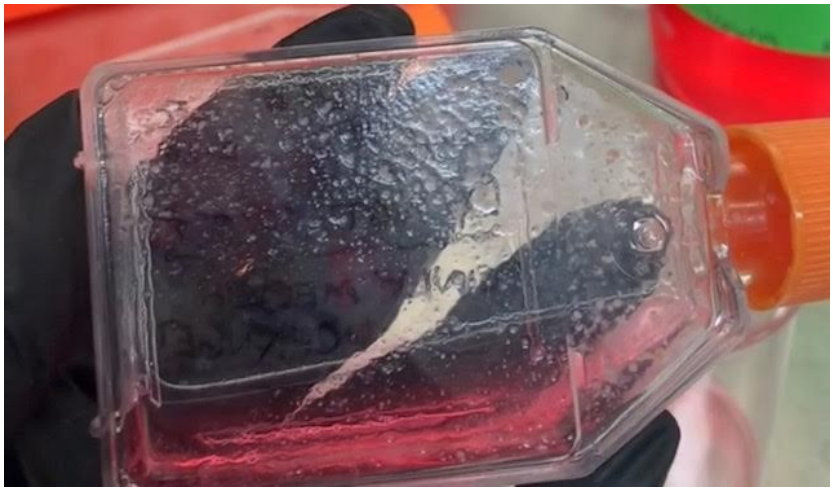

Figure 7: Photo of lab-grown adrenal cancer cells in incubated flask. As shown, there are large clusters of cells adhered to the flask, a common characteristic in adrenal cancer cells.

Once ready to test, 4 vials of frozen cells are taken out of the freezer and placed into a bath of warm water. While these vials thaw, a 15ml tube is filled with approximately 8ml of phosphate-buffered saline (PBS) where each vial of cells is emptied into after being thawed. Once all vials are in the tube, the sample is then centrifuged to create a pellet of cells at the bottom of the tube. The excess liquid is poured off to be disposed, and 10ml of PBS is added to the tube and shaken using a vortex. Once all cells are resuspended into solution, the cells are counted under a microscope using a hemocytometer to ensure the sample has a 10^6 cells/ml. These cells are then periodically spun using a vortex machine throughout testing to ensure cells are in the pipette each time they need replaced within the machine.

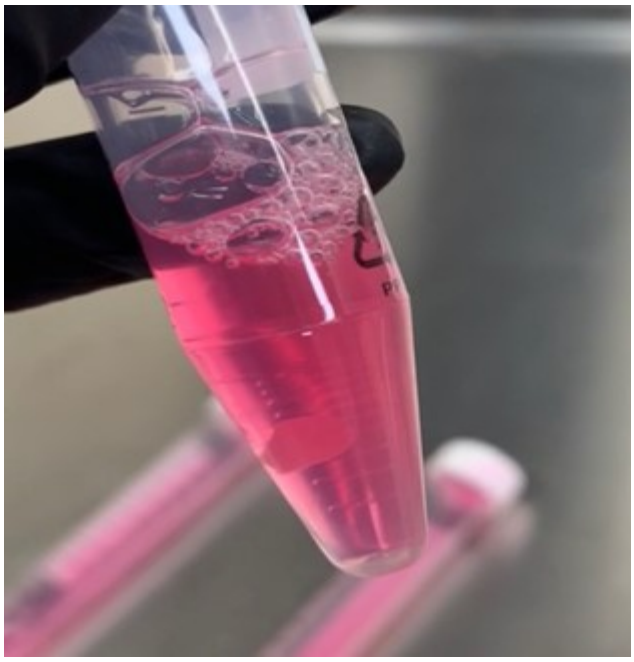

Figure 10: Photo of cells test tube upon being run through a centrifuge. The cells form one big cluster suspended in the liquid as shown.

2.2 FLOW SYSTEM FABRICATION

Flow cytometry has been implemented to detect and capture various cancer types successfully, making it a feasible idea for adrenal cancer cells as well. A photoacoustic flow cytometer uses the photoacoustic effect to look at cells individually and identify the chosen target cells. A light signal is sent through the system using a pulsed laser and an acoustic signal is detected. This signal is picked up and shown visually using an oscilloscope shown in Figure 11. This signal is then run through data analysis where each trial is compared to determine the optimal signal range. These trials are then also tested to determine if the signal shown is significant enough to be accepted, which further confirms the optimal signal and therefore confirms a detection of adrenal cancer cells.

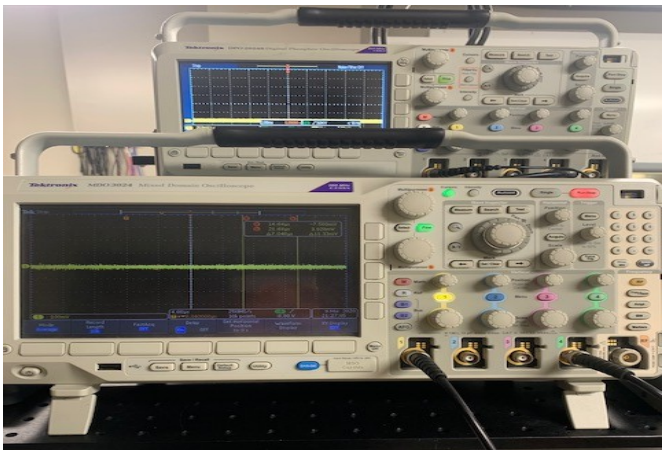

Figure 8: Oscilloscope used during testing to show signal frequency and give a visual of when cells are detected in the system.

As light travels, particles distribute through the air within its path, further weakening the light intensity as distance increases. It is important that enough laser energy reaches the flow chamber to detect the cells, as the laser energy is what is absorbed by the cell and is therefore necessary in producing the proper acoustic wave to be picked up by the oscilloscope. Because of this, it is necessary to amplify the light coming from the laser so that it is strong enough when it hits the cells in the system. This can be done using various lenses that direct and amplify the laser as it pulses. This setup includes the lens shown in Figure 12, which not only amplifies the light, but the lenses also cause the light particles coming from the laser to stay directed into one uniform path. After each lens is placed, the light energy is tested to ensure that enough light from the laser is coming from the system.

Figure 9: Lenses used for the Flow System Setup that are used to amplify and direct light from the laser to the flow chamber.

Once the lens in Figure 12 is placed properly and the energy coming out of it is tested, the lens and fiber in Figure 13 are placed and tested as well. The lens acts as a magnifying glass, amplifying the light that comes into it. The lens then directs the light to a 1000µm, 0.39 numerical aperture, optical fiber with a flat cylintrical tip and cylindrical optics. This fiber creates the desired linear beam shapes and carries the laser energy to the flow chamber, where the other end of the fiber is located.

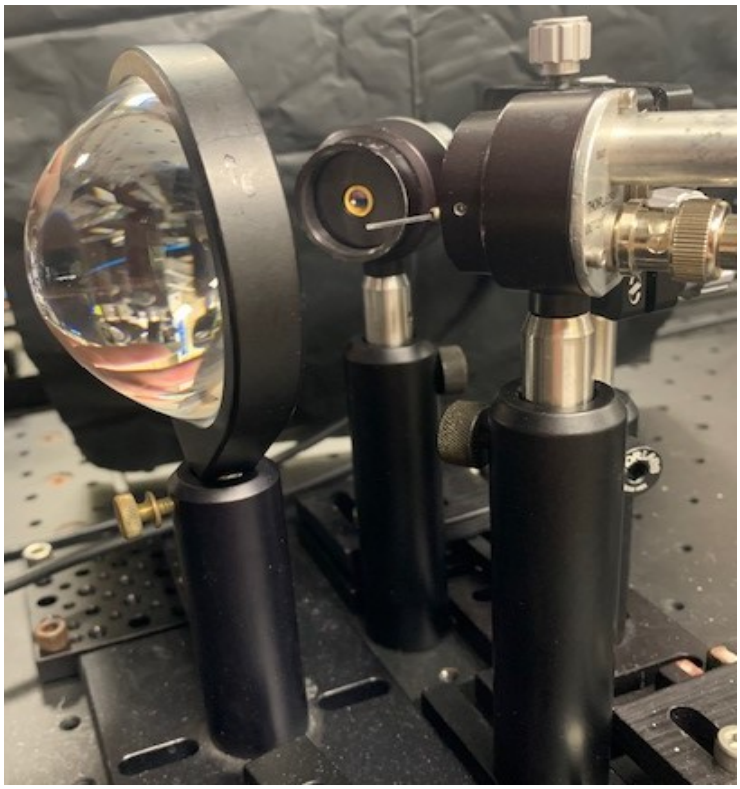

Figure 10: Second lens used to direct and amplify the laser energy, where it is then directed to the fiber shown and carried to the flow chamber.

The flow chamber used is designed and 3D printed in the lab, where they are each assembled one at a time. The flow chamber consists of the 3D housing, the tubes on the outside which are used to hold a quartz tube in place as well as direct the fluids through the chamber, and the same fiber mentioned earlier. The outside tubes ranged between 63-76mm, and the quartz tube had 10-µm-thick walls to allow the ultrasonic waves to penetrate the sample flowing through the system. The quartz tube located in the flow chamber is held by the two tubes and hot glued carefully to ensure no glue gets into the tubes or on the tube. Glue in the tube will block the fluid from flowing through the system, while flue on the tube will block the light from emitting on the cells as they flow through the quartz tube. Once the flow chamber is assembled and tested to ensure there are no fluids leaking or cracks present, it is assembled in the rest of the flow system on

top of a 2.25-MHz transducer and filled with acrylamide as shown in Figure 14. Acrylamide is a gel buffer that provides a high resolution of each cell so that the laser can easily flow to the cell and produce a sound wave. The transducer picks up on all of the sound waves produced when adrenal cancer cells are detected and sends each signal to the oscilloscope where a signal is shown.

S 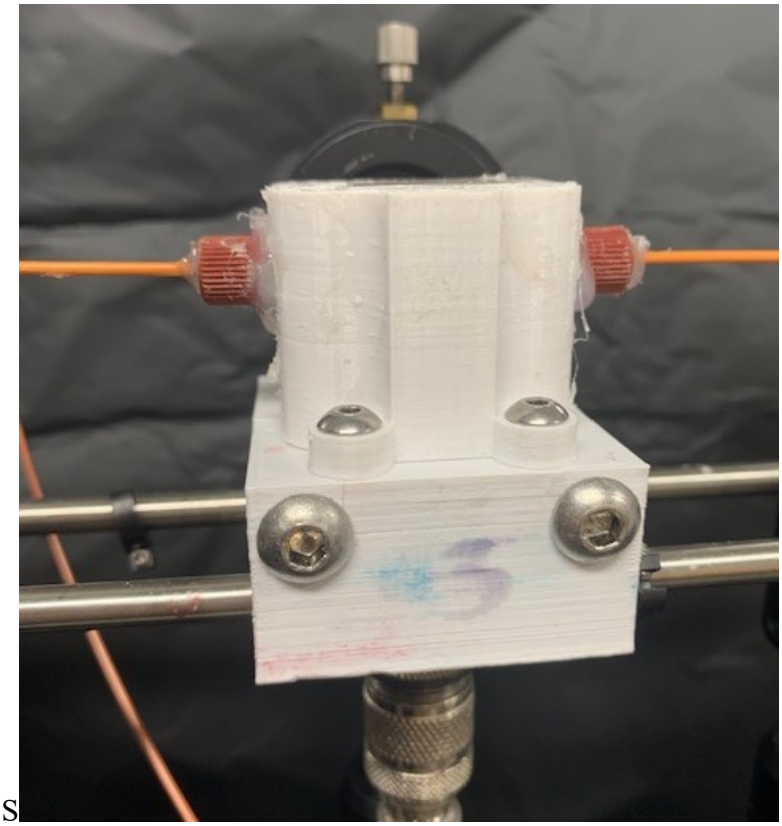

Figure 11: Working flow chamber setup used consisting of orange tubes for the fluid to flow through, a quartz tube where cells will pick up the laser energy, a fiber that directs the laser energy to the cells, and a transducer that picks up the acoustic waves and sends them back to the oscilloscope.

To simulate a pulsed flow, two tubes can be attached to the system as shown in Figure 15 below. One tube is filled with the sample being tested while the other is filled with a buffer. Each tube flows through the system, alternating solutions to create pulsed flow. This pulsed flow consists of alternating droplets of solution and droplets of the sample. By doing this, the cells are confined to the bubble they formed in, making it

easier for the laser to detect them rather than attempting to detect each cell in a constant flow of the sample. Once the fluid is done flowing through the flow chamber, it flows into a test tube attached at the other end of the tubing, where it is considered waste and is disposed of after testing.

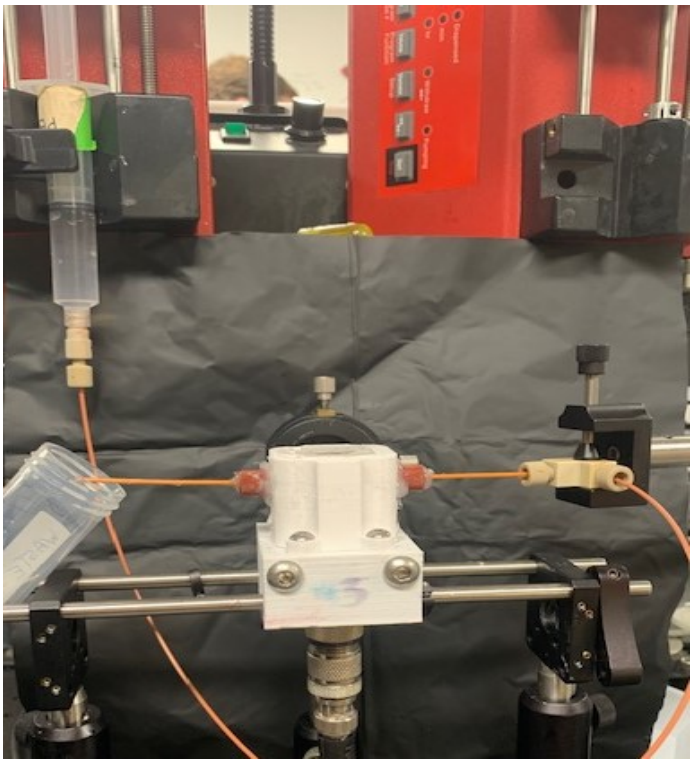

Figure 12: Set up of the flow chamber along with the pumps used to flow the sample through the system. Once fluid flows through system it flows into a waste tube to be disposed of.

2.3 TESTING

To run tests determining the optimal laser wavelength range of the adrenal cancer cells, a sample of cells suspended in 10ml PBS measuring at 10^6 cells/ml was run through the flow system at various wavelengths and their appropriate laser percentages. This concentration imitates an abundance of adrenal cancer cells within the sample, which was guessed to be enough to be detected within the system. To prevent the cells from falling

to the bottom, each time a wavelength was changed, the sample was shaken using a vortex machine before being placed in the flow chamber. Due to the photosensitivity of the cells, samples must be changed with each new wavelength to prevent photobleaching, and subsequently inaccurate results. Samples of cells were run numerous times, adjusting laser percentages, testing laser distances and placements of parts to provide optimal results, and then running cells through each wavelength until a detection was noticed. Once a detection was noticed, trials were run using all the adjustments made that led to the previous detection. Testing was run for a total of 4 trials, all containing a new sample with a cell concentration of 10^6 cells/ml. The results gathered were then run through a data analysis to determine whether there was any significant detection of adrenal cancer cells in the flow system, and if there was a significant detection, where the optimal detection range is located.

Once the detection limit was determined, tests to determine the dilution limit were completed. To determine the detection limit, it was determined that the 10^6 concentration was a sufficient starting place due to it signaling a detection in the previous experiment. Since the limit is being tested, it is only necessary to test samples with concentrations smaller than 10^6. Samples of cells having concentrations of 10^4 and 10^5 cells/ml were prepared to be run through the flow system between the wavelengths of 415 and 430nm. During these trials, adjustments were made to the laser percentages and distances between parts to ensure optimal placement with the new concentrations, however there was no significant visible detection of cells within the system. Samples of the lower concentrations were run numerous times, however none of the samples provided any

results. Therefore, it can be determined that the current flow system can detect samples containing a concentration of 10^6 cells/ml adrenal cancer cells or higher.

CHAPTER 3: RESULTS

Our initial focus was on determining the optimal wavelength for detecting the adrenal cancer cell line. To do this, we saved the data from each of the four trials to compare each trial to each other. The oscilloscope that produces the signal shown in Figure 16. The first signal on the left of the figure comes from the laser energy at the machine, producing a large signal because that is where the laser begins and is generated. The graph shows signal over time and measures the amplitude of the signal as it is detected. The signal jumps shown are given off by the transducer when an acoustic signal is detected, which is also a signal that there are adrenal cancer cells within the system. The machine shows both visual and quantifiable data that is extracted and analyzed in Matlab. The comparison of the data not only shows whether there is a trend throughout trials, but also gives an idea of whether the system is successful.

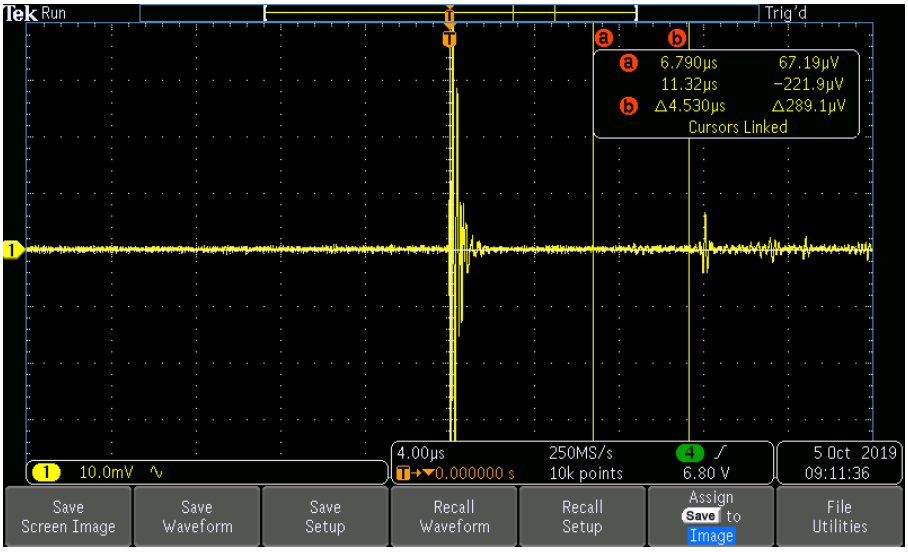

Figure 13: Real-time signal when using the flow system at 420nm wavelength. The quantified data from this signal shown from the adrenal cancer cells then gets processed in data analysis and then provides further information on how strong the detection is at each wavelength.

3.1 OPTIMIZATION OF WAVELENGTH FOR ADRENAL CANCER CELLS

Once data is quantified and compared, Figure 17a gives a visual of all 4 trials compared together. As shown, the data stands out between 400 and 500nm, meaning the optimal absorbance wavelength of the adrenal cancer cells is between those two. However, all of the trials on one graph do not narrow down this wavelength because each trial gives slightly different values. Because of this, it is important to take the data from all the samples and find the average of all of them. This will not only put all the data into one trend line consisting of all the data, but also gives a much simpler graph that easily shows the peaks in absorbance wavelengths for the cells.

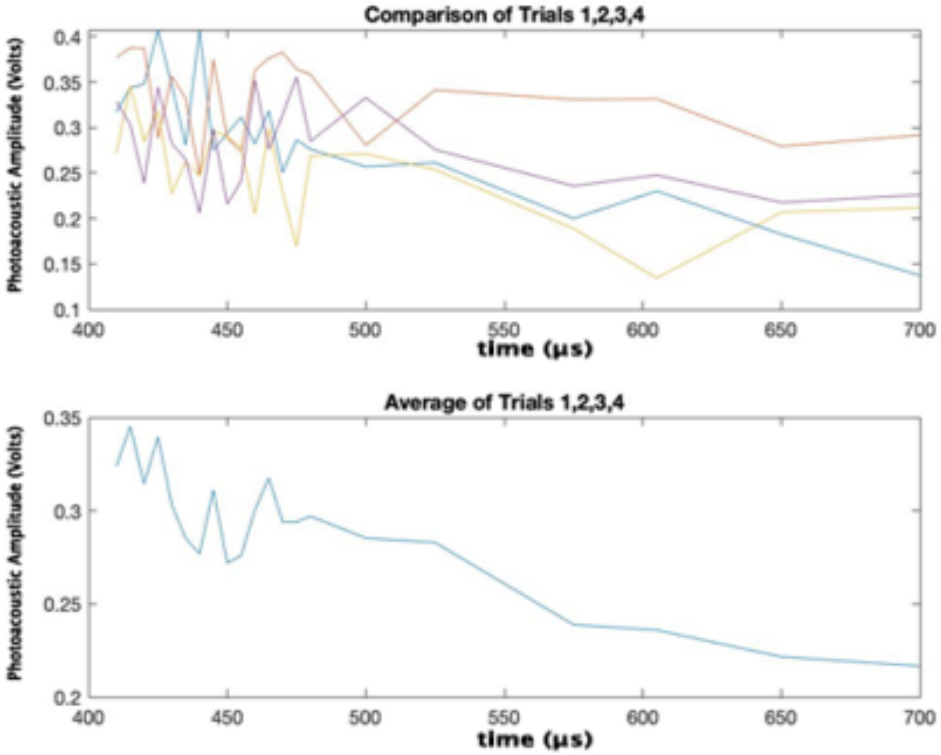

Figure 14: (a) Compares all 4 trials with each other to determine a trend in the optimal detection wavelengths of each sample. (b) Takes all the data from (a) and averages them into one single line. This line is smoother and cleaner while also giving a better visual of where acoustic signals were detected the most.

As shown in Figure 17b above, the data is run through a data analysis to determine the optimal absorbance wavelength of the adrenal cancer cells. There are substantial peaks between the wavelengths of 415 and 475nm, which is narrowed down to a smaller range than the previous assumption after studying Figure 17a. With the maximum peaks at 415 and 430nm, and a steady decline after 475nm, it becomes obvious that the adrenal cancer cells optimally absorb between 415-475nm, which is expected due to the color of the laser being blue/purple at these wavelengths. Since adrenal cancer cells are yellow in color, they should absorb blue/indigo light, which is given off in lasers

between 400-500nm. This information further validates the data acquired, and further proves that the optimal wavelength of adrenal cancer cells is within 415-475nm.

While Figure 17 validates previous assumptions that adrenal cancer cells will absorb at blue/indigo, each trial done provides a different number of cells. While they all contain a concentration of 10^6 cells/ml, differing numbers of cells in each trial slightly skews the overall data, making a true comparison of the data inaccurate. To control the cell count, the data is normalized to provide a comparison of the data within each trial if each trial had the same number of cells. The normalization of the data further controls each trial, as now the cell count is theoretically the same throughout the experiment according to the data. Once normalized, Figure 18a provides a comparison of all 4 trials. As shown, there is a major outlier within the data, as Trial 2 shows much higher signals once the cell count is normalized. While Trial 2 was comparable when testing the raw data, the control of the cell count shows that this data does not actually provide similar results to the other 3 trials. It can be seen that trials 1,3 and 4 all provide similar numerical values on the graph, while trial 2 gives results nowhere near the others.

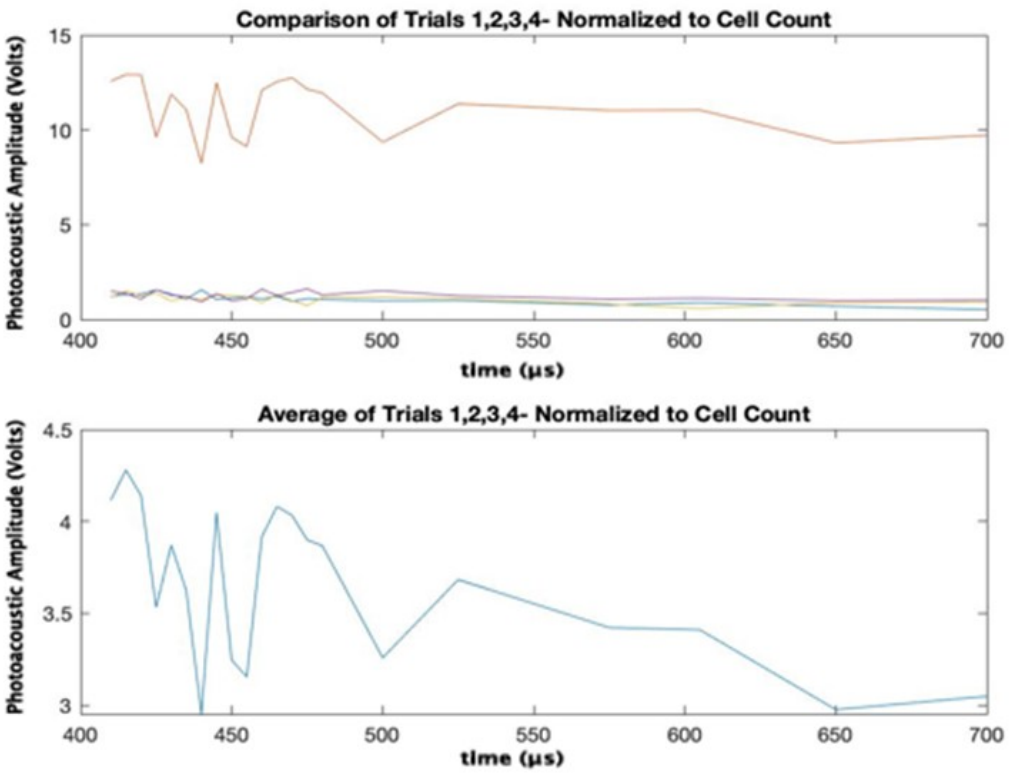

Figure 15: (a) Compares trials 1-4 after normalizing the data so that each trial theoretically has the same number of cells in its sample. (b) Takes the average of the 4 trials after normalization to further aid in determining the optimal detection range.

This outlier can further show a negative effect on the experimental data found when testing. As shown in Figure 18b, the average of the normalized data is averaged and then graphed. However, this data provides different results than that in Figure 17, as it shows there are detection peaks between 415 and 525 with possible detections up to 600nm. Not only does this information contradict the results provided in Figure 17, but this data also provides information other than what was previously assumed. While it is possible adrenal cancer cells are not optimally found in blue/indigo light as determined by the color spectrum, they also would not be absorbing light that is green or yellow in color. Adrenal cancer cells are naturally yellow in color, meaning they would reflect green and yellow light. This means that the data found after normalizing each trial is

inaccurate due to the outlying data in trial 2 and is therefore inadmissible when doing a final data analysis.

Since trial 2 provides data that does not compare to the other 3 trials, another data analysis is done on trials 1,3 and 4 after normalizing the cell count in the data. As shown in Figure 19, the data is all comparable with most peaks between 415-500 similar to Figure 17. After 500nm, the signal steadily declines, which is anticipated due to the change in color of the laser from blue to green. Again, the average of the 3 trials are done, however this data provides data closely in resemblance to the results found in Figure 17. While peaks range from 410 to about 460nm, the peaks are the strongest between the wavelengths of 410-430nm. This is significant because a laser pulsing within this range provides a blue/indigo color, which is the color assumed to be absorbed the best by the cell. After performing experiments and comparing the normalized data, it can be determined that the optimal range for detecting adrenal cancer cells when using a photoacoustic flow cytometer is between 415-430nm.

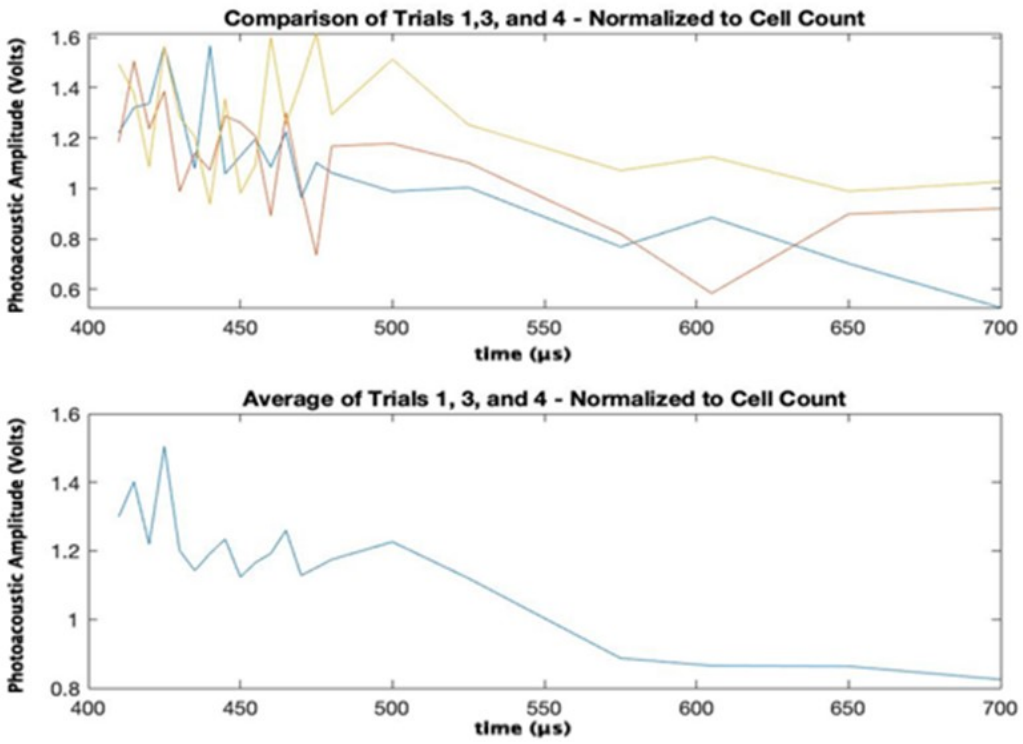

Figure 16: (a) Provides a new comparison of trials 1,3 and 4 after determining trial 2 was not accurate enough to be included in the data. (b) The average of the normalized data from trials 1,3 and 4. Optimal peaks lie between 410-430nm, which means the optimal detection range for adrenal cancer cells is within that range.

3.2 DETERMINING CURRENT MINIMUM CELL CONCENTRATION FOR FLOW SYSTEM

After determining the detection range, samples ranging in concentrations of 10^4 to 10^6 cells/ml are created and run through the system to determine the minimum concentration limit of each sample to provide a visible detection. Since the detection range is determined, each sample is run between the wavelengths of 410-430nm. However, the only samples that provide an acoustic signal are samples containing a concentration of 10^6 cells/ml. The size of the bubble formed when flowing through the system is approximately 1µl, meaning that there are about 1000 cells within each sample

bubble. All other smaller concentrations samples did not create an acoustic signal large enough for the transducer to pick up, and therefore they did not provide results. Because of this, it can be determined that the flow system currently can only detect larger samples of cells within the system, and cannot yet detect sample sizes less than 10^6 cells/ml concentration of adrenal cancer cells.

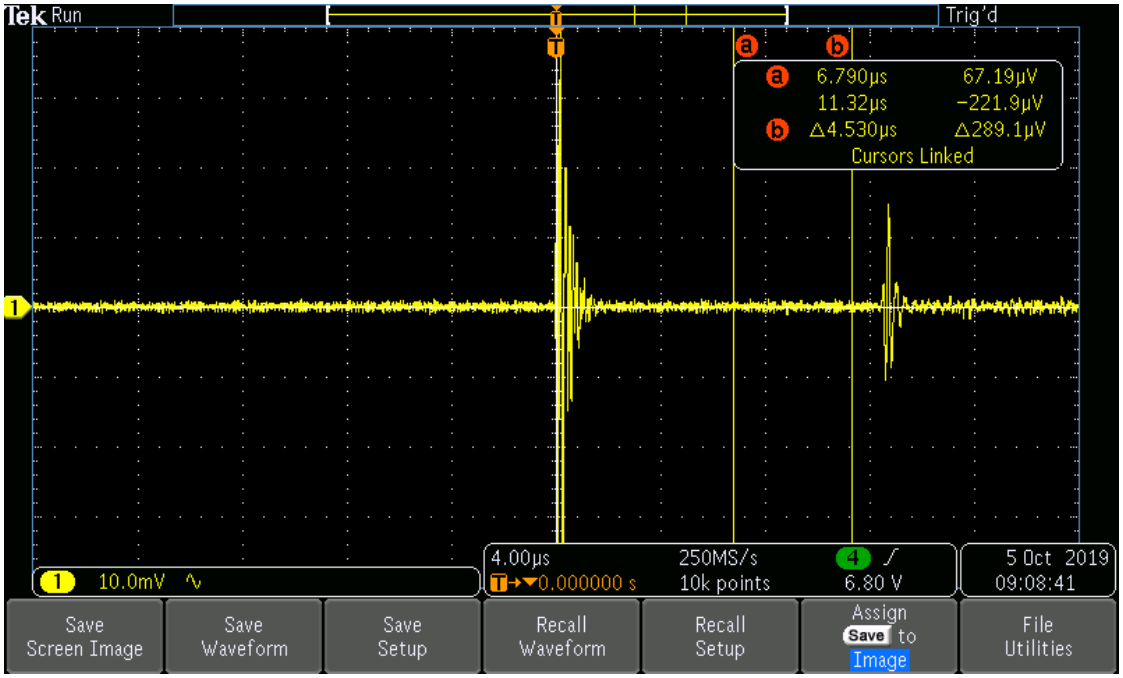

Figure 17: Visual results of a sample of 10^6 concentration of adrenal cancer cells providing a signal at 410nm.

CHAPTER 4: DISCUSSION

Upon completion of all tests, it can be seen that a significant signal is given off when running the adrenal cancer cells through the system. The optimal wavelength for detection agrees with the laws of the color spectrum, which can further confirm the results obtained during testing. When the laser is calibrated at a wavelength between 415 and 430nm while pulsing at a sample of cells with a concentration of 10^6 cells/ml adrenal cancer cells or higher in a photoacoustic flow system, the system shows repeated jumps in acoustic detection, showing that the cells are absorbing a signal at said wavelengths.

This phenomenon first developed by Alexander Bell is now successfully used in detection of adrenal cancer cells, a novel advancement in its field, as these results will aid in the completion of an early diagnostic device for the rare cancer that is not currently being used in a clinical setting.

Due to the major recent advancements in the use of photoacoustics in the detection of various cancer cell types, it became evident that the same system can be used for adrenal cancer cells as well. Early detection is crucial when detecting adrenal cancer, as the 5-year survival rate decreases drastically as the cancer progresses. Since most cases are found after large tumors are formed, a rapid early detection system would allow more patients to get routine testing, allowing for earlier treatment of the disease and therefore an increased survival rate. Because of the real time detection and the replicability, a photoacoustic flow system can provide a real-time detection, and therefore become a prime diagnostic tool when testing patients for adrenal cancer.

Because of the increased cholesterol content within adrenal cancer cells, they give off a visible yellow tint. This yellow color inferred that the cell would more easily absorb indigo/blue lasers. When looking at the wavelengths of each color, indigo/blue light falls between 400-450nm. However, when testing it is necessary to test the absorbance at all wavelengths in the spectrum to ensure that the experimental results agree with the theoretical results. As shown in the data, there are slight jumps at wavelengths larger than 430nm. However, these peaks are significantly smaller than the resulted peaks at lower absorbance wavelengths. These slight peaks completely stop around 500nm, which would be when the laser gives off a green light. This is understandable, as the laser between 450 and 500nm is a cyan color. Cyan still has a blue tint, and therefore can still be slightly

absorbed by the cells. However, as shown, the absorbance is much lower, therefore proving that these levels are not optimal for the desired cells. This then excludes testing at wavelengths giving off cyan laser light as well, which therefore means that wavelengths of approximately 450 and higher will not give an optimal absorbance, and since peaks in the data were significantly lower after 430nm,the optimal limit is then reduced even further to a small range between 415 and 430nm.

While the concentration limit for each sample is 10^6 cells/ml or higher, which is significantly higher than anticipated, there are several factors than can affect this result. One main factor that can affect the result is the strength of the laser when running cells through the flow system. While the distances between lenses was accurate and the tested laser energy was enough to give a detection, the laser energy could not be optimized due to the damage it would do to both the system and the cells. When measuring, the laser energy was at the low-end of the acceptable laser energy for detection, which could be fixed by increasing the percentage of energy the laser runs at. However, when the laser runs at a higher percentage, it becomes too damaging by burning equipment and cells. This delicate balance creates a complication as the laser energy may not be enough for the cells to absorb, but it still cannot be increased due to the damage it creates.

Another issue that could be attributed to the high concentration is how the cells react to the light as the laser pulses at it. Adrenal cells are sensitive to photobleaching, meaning that too much light causes them to lose their pigment. While the pulsed laser aids in ensuring the cells are not under direct light the entirety of the experiment, it is possible that the laser causes the cells to lose their pigment, which would therefore mean the laser is not being absorbed by any cells and therefore no acoustic signal is being

produced. This would explain why only samples with higher concentrations give a signal, as the increased number of cells allows for an increased chance that not all cells will undergo photobleaching so that an acoustic signal can be produced.

Upon completion of the experimental trials, the data received shows that a significant signal is produced when the laser is calibrated at a wavelength between 415 and 430nm while pulsing at a sample of cells with a concentration of 10^6 cells/ml adrenal cancer cells or higher in a photoacoustic flow system. This data can be used in the novel development of a photoacoustic flow cytometer for detection of adrenal carcinoma cells, aiding in the lack of early diagnosis tools available for the rare disease.

4.1 FUTURE ADVANCEMENTS

Further advancements to progress on a better early detection system for adrenal cancer include further testing using other cancer cell types such as BT-549 Human Breast Ductal Carcinoma cells and RS4 (11) Human Leukemia cells to further signify the detection from the oscilloscope is specific to adrenal cancer cells, and will not inaccurately detect other cancer cell types. Since we are basing our detection of adrenal cancer cells on the assumption that cholesterol is the marker for the cell, these two cells should not result in a detection when run through the system. This information not only further validates the results obtained in these experiments, but also further proves the novelty of creating an adrenal cancer-specific early detection system. Another further advancement includes further refining the dilution detection limit of the flow system. Doing this increases the accuracy of the flow system by decreasing number of cells needed in each specimen to trigger a detection signal.

One future test to improve the concentration would be to improve methods to remove bubbles from acoustic gel that cause the light energy to disperse, while also developing better and more permanent ways of producing flow chambers and ensuring acoustic coupling in our system. The fewer number of cells needed in each sample allows the earlier detection of adrenal cancer the patient's system. It would be optimal for the flow system to detect if there was only one cell in the system, which would aid in the earliest possible detection of patients in the future. It is also important to test the accuracy of detection within mixed populations. To study this, we can mix various cell types into one sample and run them all through the system. If the adrenal cancer cells can be detected within the mixed population, we can further improve the accuracy of the system, further proving we can distinguish cancer cells from other cells in the blood stream.

Other future developments using the information gathered include studying other cells in the blood stream to ensure they are not detected, as well as determining cell separating techniques to successfully extract the target cells from the blood stream. Once all preliminary tests are done, final tests include blind testing of patient samples to further prove the accuracy of the system, as well as to further develop credibility of the system through the use of clinical trials. Since clinical trials provide numerous different samples ranging in numerous concentrations and strains of adrenal cancer, clinical testing provides feedback on the feasibility and accuracy of the system in a real-time setting. These trials can also aid in further decreasing the concentration limit, improving precision and early detection rates using the photoacoustic flow system developed. All of these developments lead to one final goal of developing a flow system that is on the market and used in a clinical setting to help in the detection and diagnosis of adrenal

cancer in patients, finally eliminating the major issue involving high mortality rates and low early detection rates of adrenal cancer in today's clinical setting.

4.2 CONCLUSION

While significant advancements in oncology have been made over the past decade, adrenal cancer detection and treatment options have improved much slower due to the rarity and complexity of the cancer. Early detection for adrenal cancer is essential in maximizing the 5-year survival rate in patients, yet currently the majority of cases are found when tumors are too large, often pressing on other organs and spreading to other areas. To maximize survival rates and better combat the cancer, it is imperative to manufacture a system that provides assistance in the detection of adrenal cancer in the earliest stages, increasing the reliability of medications and further increasing the rate of survival.

These studies completed aid in the creation of a working photoacoustic flow system for use in early detection of adrenal cancer cells. As shown, adrenal cells are yellow in color, meaning the wavelength of laser they react best to is between 400-430nm. After completion of tests, it can be determined that the optimal wavelength for the laser within the system to be calibrated at is between 415-430nm, which aligns well with what was assumed previously. After determining the detection wavelength, the current detection limit is determined to be a 10^6 cells/ml of target cells within the system. While this means that while samples will not give off a detection unless they have a high concentration of cancer cells indicating the disease is in the later stages, this detection

limit can be decreased by doing further testing to optimize the laser energy that hits the sample and therefore allows detection signals at lower concentrations.

Further advancements using the results found during this study includes comparing these results to the results of other cell types, decreasing the detection limit and further building a replicable, working prototype for use in a clinical setting. This also includes running clinical samples through the system to ensure that the system can detect cells from actual patients rather than just lab-grown samples. These future advancements and the results from the experiments already completed will aid in the development of a novel photoacoustic flow cytometer for use in the early detection and diagnosis of adrenal cancer in patients.

APPENDIX

Adrenal Cancer Cell Culture Protocols

ALWAYS BEGIN BY EXAMINING THE FLASKS UNDER THE MICROSCOPE

1. Turn on the microscope with the power switch behind the coarse/fine focus knob
2. Remove the dust cap from the eyepiece
3. Be sure to use the 40X objective (light blue rim in middle of turret)
4. If you would like to take an image of a specimen
    a. Plug the long USB cord into the USB-C outlet on the rear of the computer tower
    b. Open the *IC Capture Program* (Found in computer toolbar next to LABView)
    c. Select the camera
    d. Pull the black metal plate on the front of the microscope towards you until it snaps into the camera position
    e. On the computer, select live mode (the *video camera icon* in the top toolbar)
    f. Focus the image using the microscope adjustment wheel
    g. Click the *camera icon* to capture an image
    h. Click *FILE* and *SAVE AS* to store the image
5. When looking under the microscope, assess the quality of the cells
    a. Notable observations can be recorded in the LOG BOOK in the rightmost column
6. Using your judgement:

    NOTE: Any free-floating cells can be pelleted down and placed back into original flask or put into new flask

    a. If there are few to no cells adhered AND the media appears red
        i. RECORD your observation in the log book and replace flask to incubator

b. If there are cells adhered with very little clear flask surface OR if there are JUST A LOT OF ADHERED CELLS
    i. SPLIT THE CULTURE
7. If you are planning to change the media or SPLIT cell cultures----- RECORD IN LOG BOOK
8. When there are more than 8 actively growing flasks in the incubator
    a. FREEZE CELLS
9. Utilize the UV light to sterilize the biological safety cabinet
10. Mechanically disinfect the biological safety cabinet with 70% ethanol or DECON Spray
    a. Be sure to clean the work surface AND walls of the cabinet

To Change the Media:

1. Remove the cell culture flasks form the incubator and place into the biosafety cabinet

Note: If there are adhered cells that are NOT ready to be split AND very few floating cells: Pour off old media, discard media, and pipet ~4 mL of fresh adrenal cancer cell culture media into flask and replace flask in incubator.

2. Pour off old media into a labeled 15 mL tube and centrifuge @ 1600 RPM for 10 minutes
3. Add 2 mL of adrenal cell culture media to each flask
4. After centrifugation, discard supernatant
5. Resuspend the pellet in ~2 mL of fresh adrenal cancer cell culture media
    a. Vortex to distribute pellet
6. Pour resuspended pellet into ORIGINAL FLASK IF NOT READY TO SPLIT or into NEW FLASK IF SPLITTING
7. BE SURE TO RECORD IN LOG BOOK

Making the Adrenal Cancer Cell Culture Media:

1. Begin with a fresh supply (500 mL unopened, *refrigerated* container) of DMEM/F:12 1X with L-Glutamine and HEPES

2. Pipet 12.5 mL of Nu Serum (need to be thawed from -20C freezer) into the base media
3. Pipet 5 mL of ITS Premix (refrigerated, small vial) into the base media
4. Pipet 5 mL of Penicillin-Streptomycin (need to be thawed from -20C freezer) into base media
5. Invert media bottle to mix contents
6. Place the suction apparatus into the hood and plug-in
7. Obtain a fresh 500-mL glass bottle and screw a filter-sterilizing apparatus to the top (Filter sterilizers are usually found above the balance work station)
8. Attach the vacuum tubing to the small outlet on the filter and turn on the vacuum
9. Pour the entire container of media into the filter and, if necessary, adjust the vacuum knob/ small switch on nozzle to yield good liquid flow
10. Label the bottle containing the filter-sterilized media with all pertinent information
    a. Keep refrigerated until needed for cell culture application

To Split the Cell Culture:

1. Pour off the old media into centrifuge tube
    a. If there are A LOT of adhered cells and you want to use more than 3 mL of TrypLE 1X Dissociation Reagent== use 50 mL tube for centrifugation
    b. If only adding 3 mL of TrypLE == use 15 mL tube
2. Add TrypLE (1x) dissociation reagent (refrigerated AND *not expired*) to each flask being split
3. Wait about 5 minutes and observe under microscope
    a. If cells are still adhered:
        i. Flick flask AND tap vigorously on table to try and manually dislodge the cells
        ii. If very few cells dissociated, add another 3 mL of TrypLE
        iii. Repeat manual maneuvers and after an additional 5 minutes, pour off the cell-TrypLE mixture into tube containing old media
            1. If cells are still adhered to flask, wash with ~5 mL of media to remove any excess TrypLE and add wash liquid

to tube------ THIS WOULD BE WHERE TO USE A 50 mL tube for this flask's contents

a. Cells may come free with wash, BUT IF NOT, add ~1 mL of fresh media NOW and ½ of pelleted mixture back into flask in STEP 7

b. If cells have dissociated

i. Pour off cell-TrypLE mixture into tube containing old media

4. Fill the tubes to the top with fresh cell culture media (either 15 mL tube or 50 mL tube depending on situation)
5. Centrifuge @ 1600 RPM for 10 minutes
6. Pour off supernatant and discard
7. Resuspend the pellet in (3 mL of fresh media for every new flask that you are creating)
    a. For Example: if the pellet is very large, then resuspend in 6 mL of fresh media, vortex, and distribute 3 mL of cell/media mixture into 2 new flasks.
8. Add extra media to each flask to obtain a *final volume ~ 4 mL* of media per flask
    a. NOTE: If using original flask with some cells still adhered, NO NEED TO ADD additional media.

To Freeze the Cells:

1. Follow the procedure to SPLIT CELLS
    a. Add enough TrypLE to get the cells to dissociate from flask
2. *Instead of resuspending cell pellet and pouring into flask:*
3. Obtain 3- 1.8 mL cryovials for each flask that is being frozen
4. Label the tube with all information found on flask
5. Resuspend the pellet in 3 mL of fresh adrenal cancer cell culture media
    a. Vortex
6. Dispense 1 mL of cell-media mixture into each cryo-tube
7. Add an additional 1 mL of sterile glycerin to each tube
    a. (Total tube volume= ~ 2 mL)
8. *Lightly* vortex the tube to mix the glycerin and cell mixture

9. Place tubes in a room-temperature Mr. Frosty filled with isopropanol
10. Place Mr. Frosty into middle compartment of -80 C freezer
11. After a day or so, transfer the cell tubes into the labeled freezer box and record appropriate information in LOG BOOK
    a. Be sure to FILL OUT THE Frozen Sample Sheet!
12. Dispose of old flask if no cells are left adhered

REFERENCES

1. American Cancer Society: "What is adrenal cancer?" National Cancer Institute: "Adrenocortical Carcinoma." Memorial Sloan Kettering Cancer Center: "Adrenal Tumors." M.D. Anderson Cancer Center: "Adrenal Tumors." Diane Reidy-Lagunes, MD, Memorial Sloan Kettering Cancer Center. UptoDate: "Adrenal Cancer."
2. Schneider DF, Mazeh H, Lubner SJ, Jaume JC, Chen H. Cancer of the endocrine system In: Neiderhuber JE, Armitage JO, Doroshow JH, Kastan MB, Tepper JE, eds. *Abeloff's Clinical Oncology*. 5th ed. Philadelphia, PA. Elsevier: 2014: 1112-1142.
3. Schneider DF, Mazeh H, Lubner SJ, Jaume JC, Chen H. Cancer of the endocrine system In: Neiderhuber JE, Armitage JO, Doroshow JH, Kastan MB, Tepper JE, eds. *Abeloff's Clinical Oncology*. 5th ed. Philadelphia, PA. Elsevier: 2014: 1112-1142.
4. Song JH, Chaudhry FS, Mayo-Smith WW. The incidental adrenal mass on CT: prevalence of adrenal disease in 1,049 consecutive adrenal masses in patients with no known malignancy. *AJR Am J oentgenol*. 2008;190:1163-1168.
5. Song JH, Mayo-Smith WM. Current status of imaging for adrenal gland tumors. *Surg Oncol Clin N Am*. 2014;23:847-861.
6. Sturgeon C, Shen WT, Clark OH, et al. Risk assessment in 457 adrenal cortical carcinomas: How much does tumor size predict the likelihood of malignancy. *J Am Coll Surg*. 2005:423-430.

7. Neuroendocrine and adrenal tumors. Plymouth Meeting, Pa.: National Comprehensive Cancer Network. http://www.nccn.org/professionals/physician_gls/f_guidelines.asp. Accessed Dec. 6, 2019.
8. Jameson JL, et al., eds. Adrenocortical carcinoma. In: Endocrinology: Adult and Pediatric. 7th ed. Philadelphia, Pa.: *Saunders Elsevier*; 2016. https://www.clinicalkey.com. Accessed Dec. 6, 2019.
9. "The Adrenal Glands." TeachMeAnatomy, teachmeanatomy.info/abdomen/viscera/adrenal-glands/.
10. "Adrenal Glands." Johns Hopkins Medicine, www.hopkinsmedicine.org/health/conditions-and-diseases/adrenal-glands.
11. Libè R, Fratticci A, Bertherat J: Adrenocortical cancer: Pathophysiology and clinical management. *Endocr Relat Cancer* 14:13–28, 2007.
12. Simons K., Ikonen E. (2000). How cells handle cholesterol. *Science* 290 1721–1726 10.1126/science.290.5497.1721
13. Hu J., La Vecchia C., de Groh M., Negri E., Morrison H., Mery L., et al. (2012). Dietary cholesterol intake and cancer. *Ann. Oncol*. 23 491–500 10.1093/annonc/mdr155
14. Silvente-Poirot S., Poirot M. (2012b). Cholesterol metabolism and cancer: the good, the bad and the ugly. *Curr. Opin. Pharmacol*. 12 673–676 10.1016/j.coph.2012.10.004

15. Floettmann JE, Buckett LK, Turnbull AV, Smith T, Hallberg C, Birch A, et al. ACAT-selective and nonselective DGAT1 inhibition: adrenocortical effects--a cross-species comparison. *Toxicol Pathol*. 2013;41(7):941–950.

16. Naing A, Habra MA, Chugh R, Ijzerman M, Phillips MD, Smith DC. ENDO. Chicago, IL: 2014. ATR-101 Phase 1 Clinical Study for Adrenocortical Carcinoma. 2014.

17. Dunn TB. 1990. Normal and pathologic anatomy of the adrenal gland of the mouse, including neoplasms. *J Natl Cancer Inst* 44:1323-1389.

18. Rosol TJ, Yarrington JT, Latendresse J, Capen CC. 2001. Adrenal gland: Structure, function, and mechanisms of toxicity. *Toxicol Pathol* 29:41-48.

19. Center, A. S. (n.d.). What Wavelength Goes With a Color? Retrieved 2 26, 2020, from National Aeronautics and Space Administration: http://scienceedu.larc.nasa.gov/EDDOCS/Wavelengths_for_Colors.html

20. "| International School of Photonics: Research: Photoacoustics: Photoacoustic Effect |." | International School of Photonics | Research | Photoacoustics | Photoacoustic Effect |, photonics.cusat.edu/Research_Photoacoustics.html.

21. Ntziachristos V (2010) Going deeper than microscopy: the optical imaging frontier in biology. *Nature Methods* **7:** 603-614. doi: 10.1038/nmeth.1483

22. Ntziachristos V et al. (2005) Looking and listening to light: the evolution of whole-body photonic imaging. *Nature Biotechnology* **23:** 313-320. doi: 10.1038/nbt1074

23. “Oscilloscope.” Merriam-Webster.com Dictionary, Merriam-Webster, https://www.merriam-webster.com/dictionary/oscilloscope. Accessed 25 Feb. 2020.

24. Sigrist M W Photoacoustic spectroscopy, method and instrumentation, Encyclopaedia of spectroscopy and spectrometry (1999) 3:1810.

25. Patel C K N, Tam A C. Pulse Optoacoustis Spectroscopy of Condensed Matter. *Physical Online Review Archive* (1981) 53:517.

26. Kinney J B, Staley R H. Applications of Photoacoustic Spectroscopy. *Annual Review of Material Science* (1982) 12:295.

27. Tam A C, Photoacoustics: Spectroscopy and other applications. *Ultrasensitive laser spectroscopy, chapter 1, New York: Academic Press*.12-50

28. Pao, Yoh-Han. Optoacoustic spectroscopy and detection. *New York: Academic Press*. (1997).

29. Mandelis A. Principles and prospective of photothermal and photoacoustic Phenomena. Progress in photothermal and photoacoustic science and technology, *Vol 1, New York: Elsevier*. (1992),455-510

30. Tam A C, Application of photoacoustic sensing techniques. Review of modern physics 58:381.

31. Nelson E T, Patel C K N. Response of Piezoelectric Transducers used in Pulsed Optoacoustic Spectroscopy. *Optics Info Base* (1981) 6:354

32. Haisch C and Niessner R. Light and Sound - Photoacoustic spectroscopy. *Spectroscopy Eur*. (2002) 14(5):10

33. Gregoriou V. Photoacoustic Spectroscopy. Available: http://nteserveur.univ–lyon1,fr/spectroscopie/ gbdo spedagogiques.html

34. Schmid T. Photoacoustic Spectroscopy for Process Analysis. Analytical and Bioanalytical Chemistry (2006); 384:1071- 1086.

35. Ball D W. The Baseline Photoacoustic Spectroscopy, *Spectroscopy* (2006); 21:14-16.

36. A. G. Bell, "On the production and reproduction of sound by light,"*Am. J. Sci.*118, 305–324 (1880).

37. A. G. Bell, "Selenium and the photophone,"*Nature* 22, 500–503 (1880).

38. A. G. Bell, "Production of sound by radiant energy,"*J. Franklin Inst*. 111,401–428 (1881).

39. A. G. Bell, "The spectrophone,"*Bull. Philos. Soc*. 4, 42 (1881).

40. Rayleigh, "The photophone,"*Nature* 23, 274–275 (1881).

41. W. C. Röntgen, "Ueber Töne, welche durch intermittirende Bestrahlung einesGases entstehen,"*Ann. Phys*. 248, 155–159 (1881).

42. J. Tyndall, "Action of an intermittent beam of radiant heat upon gaseous matter,"*Proc. R. Soc. London* 31, 307–317 (1880).

43. M. L. Veingerov, "A method of gas analysis based on the Tyndall-Röntgenoptico-acoustic effect,"*Dokl. Akad. Nauk SSSR* 19, 687–688 (1938)

44. M. L. Veingerov, "An optical-acoustic method of gas analysis,"*Nature* 158,28–29 (1946)

45. A. H. Pfund, "Atmospheric contamination,"*Science* 90, 326–327 (1939)

46. E. L. Kerr and J. G. Atwood, “The laser illuminated absorptivity spectrophone: amethod for measurement of weak absorptivity in gases at laser wavelengths,”*Appl. Opt*. 7, 915–921 (1968)

47. L. B. Kreuzer, “Ultralow gas concentration infrared absorption spectroscopy,”*J. Appl. Phys*. 42, 2934–2943 (1971).

48. A. J. Ångström, “Neue methode, das Wärmeleitungsvermögen der Körper zubestimmen,”*Ann. Phys. Chem*. 190, 513–530 (1861)

49. A. Rosencwaig and A. Gersho, “Photoacoustic effect with solids: a theoreticaltreatment,”*Science* 190, 556–557 (1975).

50. A. Rosencwaig and A. Gersho, “Theory of the photoacoustic effect with solids,”*J. Appl. Phys.* 47,64–69 (1976)

51. A. Rosencwaig, “Photoacoustic spectroscopy of solids,”*Opt. Commun*. 7,305–308 (1973).

52. W. R. Harshbarger and M. B. Robin, “Opto-acoustic effect. Revival of an oldtechnique for molecular spectroscopy,”*Acc. Chem. Res*. 6, 329–334 (1973).

53. A. Rosencwaig, “Photoacoustic spectroscopy of solids,”*Phys. Today* 28(9),23–30 (1975).

54. M. Luukkala and A. Penttinen, “Photoacoustic microscope,”Electron. Lett. 15,325–326 (1979)

55. H. K. Wickramasinghe, R. C. Bray, V. Jipson, C. F. Quate, and J. R. Salcedo,“Photoacoustics on a microscopic scale,”Appl. Phys. Lett. 33, 923–925 (1978)

56. L. Amar, M. Bruma, P. Desvignes, M. Leblanc, G. Perdriel, and M. Velghe,“Detection, d’ondes élastiques (ultrasonores) sur l’os occipital, induites par im-pulsions laser dans l’oeil d’un lapin,”*C. R. Acad. Sci. Paris* 259, 3653–3655(1964)

57. A. Rosencwaig, “Photoacoustic spectroscopy. New tool for investigation ofsolids,”*Anal. Chem*. 47, 592A–604A (1975).

58. A. Rosencwaig, “Photoacoustic spectroscopy,”*Adv. Electron. Electron Phys*. 46,207–311 (1978).

59. T. Bowen, “Radiation-induced thermoacoustic soft tissue imaging,”inProceedings 1981 Ultrasonics Symposium (IEEE, 1981), pp. 817–822.

60. T. Bowen, R. L. Nasoni, A. E. Pifer, and G. H. Sembroski, “Some experimentalresults on the thermoacoustic imaging of tissue equivalent phantom materials,”in Proceedings 1981 Ultrasonics Symposium (IEEE, 1981), pp. 823–827

61. A. A. Oraevsky, S. L. Jacques, and F. K. Tittel, “Determination of tissue opticalproperties by piezoelectric detection of laser-induced stress waves,”Proc. SPIE1882,86–101 (1993).

62. A. A. Oraevsky, S. L. Jacques, R. O. Esenaliev, and F. K. Tittel, “Laser-based optoacoustic imaging in biological tissues,”Proc. SPIE 2134, 122–128(1994).

63. M. Mehrmohammadi, S. J. Yoon, D. Yeager, and S. Y. Emelianov,“Photoacoustic imaging for cancer detection and staging,”*Curr. Mol.Imaging* 2,89–105 (2013)

64. S. Mallidi, G. P. Luke, and S. Emelianov, “Photoacoustic imaging in cancerdetection, diagnosis, and treatment guidance,”*Trends Biotechnol*. 29,213–221 (2011)

65. S. Mallidi, G. P. Luke, and S. Emelianov, “Photoacoustic imaging in cancerdetection, diagnosis, and treatment guidance,”*Trends Biotechnol*. 29,213–221 (2011)

66. Viator, J.A., Au, G., Paltauf, G., Jacques, S.L., Prahl, S.A., Ren, H., Chen, Z., & Nelson, J.S. 2002. Clinical testing of a photoacoustic probe for port wine stain depth determination. *Lasers in Surgery and Medicine*, 30(2), 141–148.

67. Viator, J.A., Komadina, J., Svaasand, L.O., Aguilar, G., Choi, B., & Nelson, J.S. 2004. A comparative study of photoacoustic and reflectance methods for determination of epidermal melanin content. *Journal of Investigative Dermatology*, 122(6), 1432–1439.

68. Weight, R.M., Viator, J.A., Dale, P.S., Caldwell, C.W., & Lisle, A.E. 2006. Photoacoustic detection of metastatic melanoma cells in the human circulatory system. *Optics Letters*, 31(20), 2998–3000.

69. Weight, R.M., Dale, P.S., & Viator, J.A. 2009. Detection of circulating melanoma cells in human blood using photoacoustic flowmetry. Pages 106–109 of: Engineering in Medicine and Biology Society, 2009. EMBC 2009. Annual International Conference of the IEEE. IEEE.

70. E. I. Galanzha, E. V. Shashkov, T. Kelly, J.-W. Kim, L. Yang, and V. P. Zharov,“In vivo magnetic enrichment and multiplex photoacoustic detection of circulat-ing tumour cells,”*Nat. Nanotechnol*. 4, 855–860 (2009)

71. Galanzha, Ekaterina I., et al. “In Vivo Liquid Biopsy Using Cytophone Platform for Photoacoustic Detection of Circulating Tumor Cells in Patients with Melanoma.” *Science Translational Medicine, American Association for the Advancement of Science*, 12 June 2019, stm.sciencemag.org/content/11/496/eaat5857?utm_source=TrendMD&utm_medium=cpc&utm_campaign=TrendMD_1.

72. Robert H. Edgar, Justin Cook, Cierra Noel, Austin Minard, Andrea Sajewski, Matthew Fitzpatrick, Rachel Fernandez, John D. Hempel, John A. Kellum, John A. Viator, "Bacteriophage-mediated identification of bacteria using photoacoustic flow cytometry," *J. Biomed. Opt*. 24(11) 115003 (22 November 2019) https://doi.org/10.1117/1.JBO.24.11.115003